JOURNAL OF AIRCRAFT
Vol. 37, No. 2, March–April 2000

Aerodynamics of Gurney Flaps on a Single-Element High-Lift Wing

David Jeffrey* and Xin Zhang†
University of Southampton, Southampton, England S017 1BJ, United Kingdom
and
David W. Hurst‡
Glasgow University, Glasgow, Scotland G12 8QQ, United Kingdom

The trailing-edge region of a single-element wing fitted with Gurney flaps has been studied. Measurements include surface pressure, force, and velocity by laser Doppler anemometry (LDA). The mean-velocity vectors and streamlines suggest a twin vortex structure downstream of the Gurney flap. Spectral analysis of the LDA data indicates that the wake consists of a von Kármán vortex street of alternately shed vortices, and this flow structure is confirmed by smoke visualization of the flow downstream of the Gurney flap. The vortex shedding increases the trailing-edge suction of the aerofoil, whereas the upstream face of the device decelerates the flow at the trailing edge of the pressure surface. These two changes result in a pressure difference acting across the trailing edge, and it is this that generates the increase in circulation.

Nomenclature

A	= aspect ratio
b	= wing span
C_D	= drag coefficient
C_{D_0}	= zero-lift C_D
C_L	= lift coefficient
$C_{L_{\max}}$	= maximum C_L
C_p	= pressure coefficient
c	= wing chord
c_{d_0}	= two-dimensional zero-lift drag coefficient
c_f	= skin-friction coefficient
d	= base dimension
f_p	= principal frequency
h	= Gurney flap height
L/D	= lift-to-drag ratio
l_f	= formation length
Re_c	= Reynolds number based on c
R_θ	= Reynolds number based on θ
Sr	= Strouhal number
U_∞	= freestream velocity
u, v, w	= velocity components in x, y, and z axes system
$\bar{u}, \bar{v}, \bar{w}$	= time-averaged velocity components
u', v', w'	= perturbation velocity components
x, y, z	= coordinate system: x positive downstream, y positive to starboard, z positive up
α	= incidence
γ	= singularity strength
ζ	= vorticity
η	= nondimensional span, $\eta = \lvert 2y/b \rvert$
θ	= boundary-layer momentum thickness

Introduction

THE Gurney flap is a mechanically simple device, consisting of a short strip, fitted perpendicular to the pressure surface along the trailing edge of a wing. It can have a relatively powerful effect on the aerodynamics of a wing, increasing lift at a given incidence with only a small change in the stalling incidence, resulting in an increase in $C_{L_{\max}}$. The blend of simplicity and efficacy make the device popular in motor racing, where it is used to increase downforce and, hence, cornering speeds. Gurney flaps were first used in this manner in the late 1960s by the American race car driver and team owner, Daniel Gurney, who is generally credited with inventing the device that now bears his name.

In race car applications, the height of the Gurney flap is typically in the range of 1–5% of aerofoil chord. Figure 1 illustrates a 4% device, fitted to the single-element wing used in this investigation.

The earliest reference to a Gurney flap by that name was made by Liebeck,[1] but similar devices were evaluated prior to the 1960s, for example: short split flaps deployed at 90 deg (Ref. 2), fixed trailing-edge strips,[3] and external spars at the trailing edge.[4]

Since the introduction of Gurney flaps, their overall effects have been well documented, (e.g. Liebeck[1] and Myose et al.[5]), but the actual causes of these increases in C_L are less well understood.

The first discussion of the flow around the Gurney flap was presented by Liebeck,[1] who hypothesised a short region of separated flow directly upstream of the Gurney flap, with two counter-rotating vortices downstream. He described these vortices as having a turning effect on the local flowfield. Neuhart and Pendergraft[6] observed similar vortex structures in a water tunnel, but at a relatively low Reynolds number ($Re_c = 8.6 \times 10^3$). At this Reynolds number the wake of the aerofoil with no Gurney flap fitted was unstable, making it difficult to identify any flow instabilities that were caused by the Gurney flaps. All of the existing Reynold-averaged Navier–Stokes (RANS) computational studies of the flow around Gurney flaps (for example, those performed by Jang et al.[7]) have presented time-averaged results and give no information on any flow instabilities.

Thus, although the Gurney flap has been in use for some time, the published experimental and computational results do not fully describe the physics of the flow around the device and cannot totally explain why the Gurney flap generates increases in lift.

This paper presents selected results from a recent study into the aerodynamics of the Gurney flap,[8] which was performed at the University of Southampton. The results presented here illustrate the large-scale unsteady and time-averaged flow features caused by fitting a Gurney flap to a single-element aerofoil. By establishing these features it is possible to develop a greater understanding of why such a basic device can have such a profound effect on the forces generated by a wing.

Received 19 May 1999; revision received 15 September 1999; accepted for publication 27 September 1999.

*Penske Research Student, School of Engineering Sciences; currently, Aerodynamicist, British American Racing, Brackley, Northans NN13 7BD, U.K.
†Senior Lecturer, School of Engineering Sciences. Senior Member AIAA.
‡Senior Lecturer, Department of Aerospace Engineering.

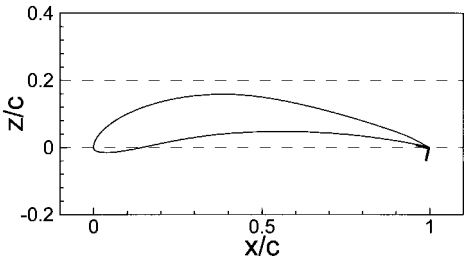

Fig. 1 Section e423 with 4% Gurney fitted, $\alpha = 0$ deg.

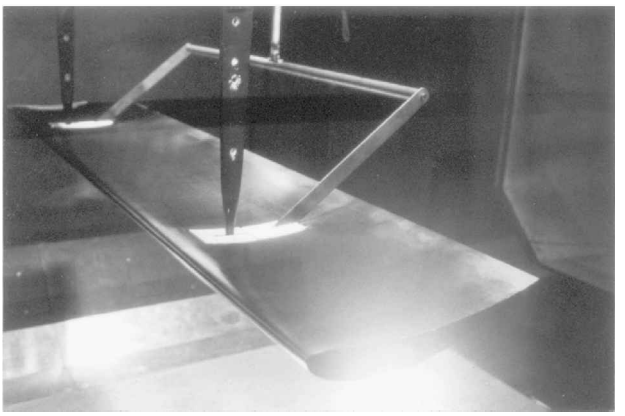

Fig. 2 Installation of model in wind tunnel.

Experimental Setup

The experiments described here were performed as part of a series of tests investigating the generic effects of Gurney flaps and were preceded by tests on a similar wing of symmetrical NACA 0012 section and followed by experiments on a double-element wing similar to those used on race cars.[8] In this paper, results are presented for an untwisted constant-chord wing of finite span that has an Eppler e423 section.[9] The Eppler section, illustrated in Fig. 1, was chosen because it has been optimized for high lift and shares some features with typical race car wing elements, for example, a significant degree of camber on the pressure surface.

This wind-tunnel model had an aspect ratio of $A = 5.0$ and a chord of $c = 0.32$ m. Figure 2 illustrates this model installed in the University of Southampton 2.1×1.7 m tunnel. The model is supported, pressure surface uppermost, by two vertical supports located at 57% semispan from the wing centerline and by a third strut located on the centerline downstream of the wing.

Full-span Gurney flaps of $h/c = 1$, 2, and 4% were manufactured from 1.3-mm-thick aluminium sheet bent to shape. A 0.5% h/c Gurney flap was made from 1.6-mm square spruce strip. These device heights are typical of those used on race car wings. The Gurney flaps were fitted normal to the local curvature, on the same surface as the tunnel supports and pitch arms.

The model had 39 chordwise taps, located 50 mm from the centerline of the wing ($\eta = 0.0625$) and a total of 10 spanwise taps on each surface at the quarter chord. A limited number of measurements were also made of the pressures acting on the upstream and downstream faces of the Gurney flaps. For the 2 and 4% devices, these measurements were obtained by fitting lengths of 1.5-mm o.d. hypodermic tubes along the two faces of the Gurney flaps (resulting in an increase in the thickness of the devices to 3.3 mm). A 1% Gurney flap was created by using four tubes to form a device with a square cross section. These tubes all had a 0.7-mm tap in line with the chordwise wing taps. Surface-pressure measurements indicated that the increased thickness of the tapped Gurney flaps had only a marginal effect on the changes in chordwise loadings generated by the thinner, untapped, devices.

Laser Doppler anemometry (LDA) surveys near the trailing edge of this wing were performed using a three-component system installed in the University of Southampton's 3.5×2.5 m wind tunnel. For these experiments the freestream turbulence level in the 3.5×2.5 m tunnel was of the order of 0.3%.

All of the other experiments were performed with the model in the University's 2.1×1.7 m wind tunnel, which has a freestream turbulence level of the order of 0.2%.

With the exception of the smoke-flow visualization, these experiments were performed at a freestream velocity of $U_\infty = 40$ ms^{-1}, which gave Reynolds numbers in the range $Re_c = 0.75$–0.89×10^6. (The variation in Reynolds number for each test was caused by variations in ambient pressure and temperature.) The smoke-flow experiments were performed at the reduced velocity of $U_\infty = 10$ ms^{-1}, which gave Reynolds numbers in the range $Re_c = 0.26$–0.28×10^6. For all of these tests, transition was not forced on either surface, although oil-flow visualizations revealed that the pressure taps triggered localized premature boundary-layer transition. No trip wires or wall treatments were applied to the wind-tunnel walls.

The forces, measured from the overhead balance, have been corrected to free-air wind-axes coefficients, and all quoted incidences are measured relative to the $z/c = 0.0$ axes shown in Fig. 1. Incidence corrections derived from the force measurements have also been applied to the surface pressures, but no other corrections have been made to the measured pressures, nor have any been made to the LDA results.

In the measurements of C_L and C_D, uncertainties in force balance readings, data-acquisition system, and incidence settings all contributed to the overall uncertainties. An uncertainty analysis gives typical first-order uncertainties of ± 0.0087 in the lift coefficient and ± 0.00078 in the drag coefficient. The surface pressure were measured using a Scanivalve system by averaging 20 samples taken over 0.5 s, and a Scanivalve zero operate calibrate system averaging 270 samples taken over 7 s. An uncertainty analysis gives a typical total uncertainty of ± 0.013 in C_p. Uncertainties in $\bar{u}/U_\infty$, $\bar{v}/U_\infty$, and $\bar{w}/U_\infty$ measurements are ± 0.003, ± 0.011, and ± 0.012, respectively.

Experimental Results

Measured Forces

Figure 3 presents measured forces for the model with a range of Gurney flaps fitted at the trailing edge. All of the Gurney flaps

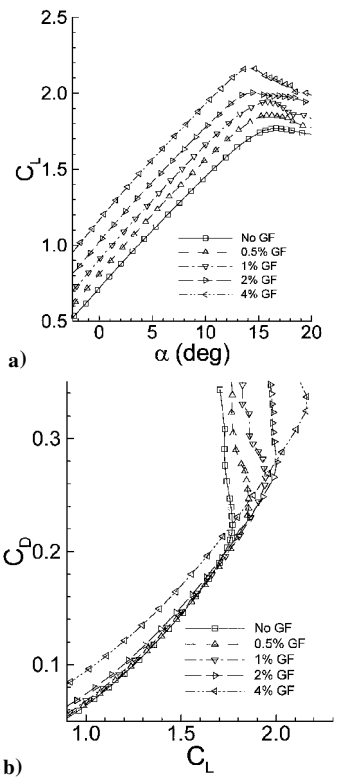

Fig. 3 Forces: a) C_L vs α and b) C_D vs C_L.

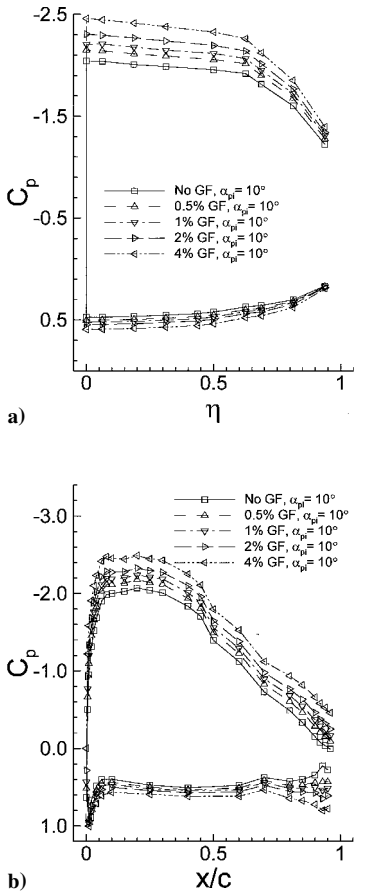

Fig. 4 Surface pressures at α = +10.0 deg: a) spanwise and b) chordwise.

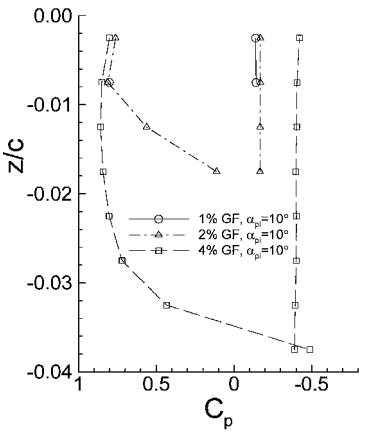

Fig. 5 Gurney pressures.

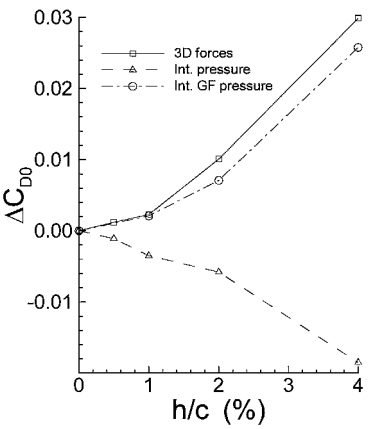

Fig. 6 Comparison of integrated and measured Δc_{d_0}.

increase the lift at a given prestall incidence and increase the drag at most values of C_L, leading to reductions in the maximum lift-to-drag ratio. Fitting a Gurney flap results in a sharper stall by extending the linear portion of the C_L vs α curves and increasing the loss of C_L in the stall. Despite a reduction in stalling incidence the Gurney flaps still increase $C_{L_{\max}}$.

Surface Pressures

Surface pressures measured at the quarter-chord taps are presented in Fig. 4a. At unstalled incidences the loadings remain broadly constant across the central portion of the wing. It, therefore, appears that, in terms of loadings, there is quasi-two-dimensional flow up to half semispan. The Gurney flaps generate an increase in loadings across the whole span of the wing, on both surfaces.

Typical chordwise distributions of surface pressure are presented in Fig. 4b. These show that the Gurney flaps increase the overall loadings, as well as the maximum suction. There are increases in the trailing-edge suction and the trailing-edge pressure, resulting in a finite pressure difference at the trailing edge of the aerofoil.

If the suction-surface recoveries are replotted in their canonical form,[10] it is found that at low incidences (up to $\alpha = 11$ deg) the Gurney flaps provide protection against a trailing-edge separation by reducing the pressure recovery demands, which explains the longer linear portion in the C_L vs α curve. Above this incidence the Gurney flaps promote a localized suction peak near the leading-edge peak, pushing the boundary layer closer to separation and reducing the stalling incidence. These trends were confirmed using oil-flow and tuft techniques to visualize the surface flow.

Gurney Flap Pressures

Figure 5 presents values of C_p acting on the faces of the 1, 2, and 4% Gurney flaps at $\alpha = +10.0$ deg. The distributions plot z/c against C_p, with positive pressures on the left-hand side and with the edge of the Gurney flap nearest the wing surface ($z/c = 0.0$) at the top. The results for the 1% Gurney flap show only three taps because of problems with the fourth.

For all three devices there is a region of positive pressure acting on the upstream face of the Gurney flap and a suction on the downstream base. The base suction is relatively constant across the downstream face for any given device height, but the magnitude of this increases with height. In contrast, the height of the device has a relatively weak effect on the maximum pressure acting on the upstream face of the device.

Figure 6 compares values of two-dimensional Δc_{d_0} derived from integrated surface pressures, including and excluding the loadings on the Gurney flap, with three-dimensional values estimated from the force measurements. When the pressures acting only on the surface of the aerofoil are integrated, the results indicate that the Gurney flaps reduce c_{d_0}. In contrast, when the Gurney flap pressures are included, positive increments in c_{d_0} are observed that are similar to those derived from the measured forces. This implies that the increase in drag caused by fitting a Gurney flap is largely caused by the normal-pressure drag acting on the two faces of the device.

LDA Measurements

Typical time-averaged results from the LDA surveys are presented in Figs. 7 and 8 for the wing at $\alpha = 0$ deg, fitted with a 4% Gurney flap. These LDA measurements were obtained at the same spanwise station as the surface pressures. The area surveyed was split into a number of grids that were designed to define the overall features of the flow in the trailing-edge region and wake regions using the minimum number of points.

The flow was seeded using atomized oil, with particulates 3 μm in diameter, introduced upstream of the wing using a rake. This was found to give high enough data rates in the region directly downstream of the Gurney flap without compromising the aerodynamic characteristics of the wing.

In addition to the results presented here, a more detailed survey was performed investigating the boundary layer of the aerofoil with no Gurney flap fitted at $x/c = 0.9$ on the pressure surface. The results

Table 1 Measured velocity and pressure data

GF (h/c), %	α, deg	$\zeta c/U_\infty$ Min	$\zeta c/U_\infty$ Max	$\overline{u'^2_{max}}/U_\infty^2$ Suction surface	$\overline{u'^2_{max}}/U_\infty^2$ Pressure surface	$\overline{w'^2_{max}}/U_\infty^2$	f_p, Hz	Sr	d/l_f	C_{SS} Trailing Edge
None	0	−30.9	54.1	——	0.112	0.012	——	——	——	0.013
1	0	−110.5	272.6	0.031	0.058	0.043	1120	0.081	0.53	−0.197
2	0	−89.1	185.9	0.044	0.074	0.092	900	0.137	0.57	−0.305
4	0	−70.0	118.1	0.087	0.146	0.288	450	0.141	0.94	−0.503
4	3	−55.2	104.9	0.077	0.164	0.222	465	0.146	0.67	−0.506
4	5	−44.9	78.5	0.065	0.117	0.184	450	0.143	0.73	−0.503
4	8	−37.5	86.6	0.063	0.130	0.184	430	0.135	0.50	−0.475
4	10	−28.2	65.7	0.075	0.093	0.136	310	0.098	0.39	−0.458

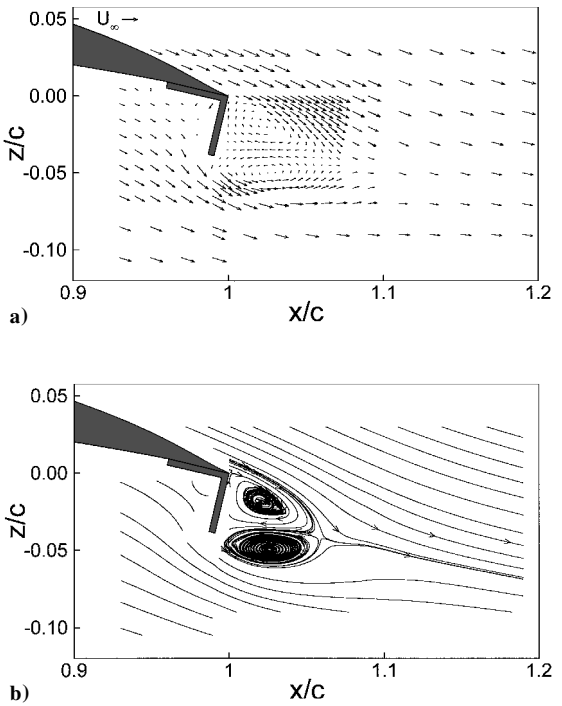

Fig. 7 Time-averaged LDA results: a) mean-velocity vectors, and b) streamlines (4% Gurney, α = 0.0 deg).

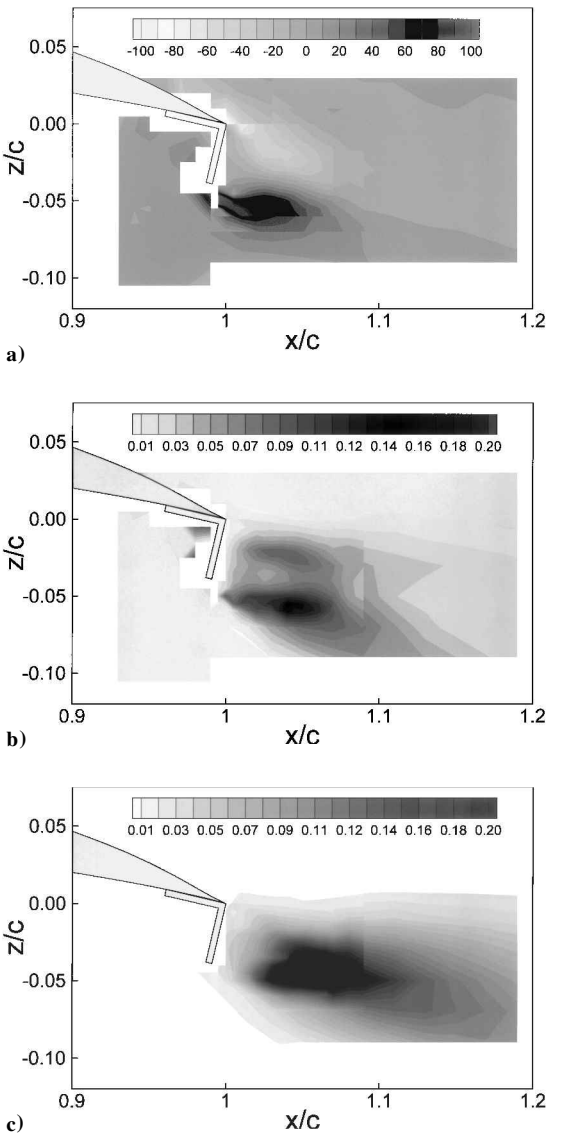

Fig. 8 Time-averaged LDA results: a) contours of planar vorticity, $\zeta c/U_\infty$, b) contours of $\overline{u'^2}/U_\infty^2$, and c) contours of $\overline{w'^2}/U_\infty^2$ (4% Gurney, α = 0.0 deg).

indicated a 99% boundary-layer thickness of 0.025 z/c and a skin-friction coefficient, estimated using a Clauser plot of $c_f = 0.0038$.

Figures 7 and 8 include mean-velocity vectors, streamlines, vorticity, and mean-square perturbation velocities for a region near the trailing edge of the wing. The vorticity at any point in the x–z plane, $\zeta = \partial w/\partial x - \partial u/\partial z$, was estimated using one-sided differences at the edges of each LDA measurement grid and center differences for interior points. The resulting values were nondimensionalized using the freestream velocity and aerofoil chord. The mean-square perturbation velocities (for example, $\overline{u'^2}$ where $u' = u - \bar{u}$) were measured in the wind axes system and nondimensionalized using the square of the freestream velocity.

Although not plotted here, LDA surveys were also performed downstream of the e423 wing fitted with 1 and 2% Gurneys and at different incidences with the 4% device. The maximum and minimum values of vorticity and perturbation velocities are listed in Table 1 for all these cases.

In Fig. 7 the time-averaged velocity vectors and the resulting streamlines show two distinct counter-rotating vortices directly downstream of the Gurney and an offsurface stagnation point where the streamlines bounding the vortex region meet to form the wake. This pattern matches that first hypothesized by Liebeck[1] and is similar to those predicted by time-averaged RANS computational methods for aerofoils with Gurney flaps fitted.[7] Twin-vortex patterns are also evident in the RANS simulations of flow around aerofoils with blunt trailing edges.[11]

The measurement points in the recirculating region are not spaced closely enough to draw any conclusions over the finer features in this region. It is, therefore, not possible to confirm if the time-averaged flow shares features of an attached boundary-layer flow, such as having an inertial sublayer (log-law region), or if the features are more closely related to those for reversed flow in separated boundary layer.[12] For similar reasons, it is not possible to estimate the skin friction acting on the upstream and downstream faces of the Gurney.

In the corner between the upstream face of the Gurney flap and the pressure surface of the aerofoil, there is some evidence of a recirculating separation bubble. Most notably, there is a single point with a large velocity away from the corner. Similar velocity components were also found for other device heights and at other incidences, and so this appears to be a genuine feature of the flow, rather than a measurement anomaly. If there is a recirculation bubble it is highly localized, and the limited results in this region mean the dimensions of this bubble cannot be firmly established.

Spanwise velocities were also extracted from the LDA results. Momentum integrals were performed using these velocities, and the results indicated that when no Gurney flap was fitted the average momentum exiting the surveyed region in a spanwise direction was approximately 3% of the axial momentum exiting the downstream edge of the region. With the 4% Gurney fitted, this figure rose to 6% for the whole region surveyed. At the downstream edge of this region, the spanwise momentum was also approximately 6% of the axial, indicating that the increase in spanwise flow caused by the Gurney flap was not restricted to the recirculating region.

The contours of vorticity plotted in Fig. 8a show two concentrations of opposite signs downstream of the Gurney flap, with peak values that lie on the streamlines that bound the vortical region. In general, the vertical gradients of axial velocity, $-\partial u/\partial z$, form the dominant component of the vorticity, but the weaker concentrations of $\partial w/\partial x$ are typically in the same locations. There are also two distinct concentrations of $\overline{u'^2}/U_\infty^2$ downstream of the Gurney flap, but only one, stronger, concentration of $\overline{w'^2}/U_\infty^2$.

The vortex structures do not scale directly with height of the Gurney flap: The suction-surface vortex appears disproportionately large for the smaller devices, as is the spacing between the two vortices. This results in the pressure-surface vortex having higher velocity gradients and, hence, stronger peak vorticity. Reducing the height of the Gurney flap also reduces the size and magnitude of the concentrations of the two mean-square perturbation velocities. Note that the values listed in Table 1 show a large maximum value of $\overline{u'^2}/U_\infty^2$ for the wing with no Gurney flap fitted. This represented a localized region of high turbulence, corresponding to a trailing-edge separation.

As the incidence of the wing fitted with the 4% Gurney flap is increased, the points of zero mean velocity at the center of the counter-rotating streamlines move downstream relative to the trailing edge. The pressure-surface, zero-velocity point also moves downstream relative to that for the suction surface. Although the length of the vortex structure increases, the overall depth of the vortex structure is not greatly affected, and so the vortices appear more stretched than at lower incidences. Increasing the incidence weakens the maximum values of positive and negative vorticity while extending the length of the contours and increasing the separation between the maxima. The concentrations of both components of the perturbation velocities also move further downstream, and the maxima are reduced.

Time-averaged streamlines, vorticity contours, and concentrations of $\overline{u'^2}/U_\infty^2$ and $\overline{w'^2}/U_\infty^2$ similar to those plotted in Figs. 7 and 8 were also observed from surveys performed downstream of a 0012 wing fitted with a 4% Gurney flap and for an isolated flat plate of the same height.[8] Other researchers, for example, Cantwell and Coles,[13] have shown that similar time-averaged flows are found downstream of vortex-shedding bodies.

Spectral Analysis

Traditionally, a Fourier method would be used to derive power spectra for regularly sampled signals. LDA measurements are acquired with nonuniform time spacing, and so instead the Lomb periodogram method[14] was used because this is specifically designed for randomly spaced data.

There are no distinct peaks in the power spectra for the e423 wing with no Gurney flaps. In contrast, downstream of the wing with Gurney flaps fitted, single peaks were observed at periodic frequencies f_p that remain broadly constant in a region downstream of the trailing edge. Although the Lomb periodogram method is capable of discerning more than one peak in the power spectra, multiple frequencies were not evident downstream of the Gurney flaps. Because no peaks were evident in the seeded flow directly upstream of the wing, it appears that these peaks represent periodicity introduced by the Gurney flaps and are not indicative of some seeding phenomenon.

Fig. 9 Smoke-flow visualization, flow from left to right, U_∞ = 10, α = 0.0 deg.

Table 1 lists f_p for the different cases tested that represent the statistical mode of f_p for the measurement points inside the periodic flow. Table 1 also includes estimates of the Strouhal number, $Sr = f_p d/U_\infty$, where d is the base dimension, that is, measured normal to the $z/c = 0.0$ chordline and including the trailing-edge thickness. From Table 1, it can be seen that reducing the device height increases f_p, from 450 Hz for the 4% Gurney flap to 1120 Hz for the 1% device, but reduces the Strouhal number from $Sr = 0.141$ to 0.081. In contrast, increasing the incidence from $\alpha = 0$ deg to +10 deg reduces both the frequency, from 450 to 310 Hz, and the Strouhal number, from $Sr = 0.141$ to 0.098. For the larger devices at low incidences these Strouhal numbers are of a similar order to those for vortex-shedding bodies, for example, $Sr = 0.135$ for flat plates.[15]

Assuming no noise, the amplitude of any periodic instability in the flow is given by the perturbation velocity. Experimental results indicate that for the flow downstream of the Gurney flap there is a broad agreement between the actual amplitude and that predicted from the values of $\overline{w'^2}$ derived from the LDA results. The maxima listed in Table 1 should, therefore, give a good indication of the relative amplitudes of the flow instability for the different cases tested.

It can be seen from Table 1 that increasing the height of the Gurney flap increases the maximum values of $\overline{w'^2}$ and, hence, the amplitude of the flow instability, The overall trend for the wing fitted with the 4% Gurney flap is that increasing the incidence reduces the amplitude of the instability.

Smoke-Flow Visualization

Photographs were taken in the 2.1 × 1.7 m wind tunnel showing the smoke-flow patterns downstream of the wing with and without Gurney flaps fitted. The single-filament smoke probe was placed at approximately the same spanwise station at which the LDA measurements and surface pressures were obtained.

When no Gurney flap is fitted no coherent structure is evident, but if a Gurney flap is fitted a wake of alternate vortices forms downstream of the trailing edge. This is illustrated in Fig. 9, which shows the wake developing downstream of the 4% Gurney flap. In this instance the vortex spacing is approximately 20% chord. For a 2% Gurney flap similar patterns are evident, but with a spacing of the order of 10% chord. If it is assumed that the rate of change of position of the fully formed vortices matches those for other vortex-shedding bodies, typically of the order of 75% of the freestream velocity,[13] these spacings yield Strouhal numbers of $Sr \approx 0.15$ for both devices.

Discussion of Results

Vortex Shedding by the Gurney Flap

The results for the wing with no Gurney flap fitted indicate a wake with no strong instabilities. This is consistent with the hot-wire surveys performed by other researchers, who have not reported any vortex shedding downstream of aerofoils with sharp trailing edges, even for aerofoils with separated flow.[16,17]

The LDA surveys reported here indicate that although the time-averaged flow downstream of the Gurney flap matches Liebeck's hypothesis,[1] the instantaneous flow structure actually consists of a

wake of alternately shed vortices. This vortex shedding is confirmed by the smoke-flow visualizations. To explain how this change in the wake contributes to the increases in C_L generated by fitting a Gurney flap, it is first necessary to understand the process of vortex shedding for a typical bluff body.

In a two-dimensional, vortex-shedding flow the boundary layers on a bluff body separate at some point to form two shear layers of opposing vorticity. The generally accepted mechanism by which these separating shear layers interact to form a von Kármán vortex street was first postulated by Gerrard.[18] The first stage in this shedding cycle begins as the separating shear layer on one side of the body rolls up to form a vortex. As it does so, it draws the separating shear layer over from the other side of the body. This second shear layer contains vorticity of opposing sign, and as it crosses the wake centerline it cuts off the supply of vorticity to the shear layer that is rolling up. At this point, the vortex is shed and moves downstream, while the shear layer on the opposite side starts to roll up, repeating the process.

With the Gurney flap the offsurface edge provides a fixed separation point for the pressure-surface shear layer, and this interacts with that separating from the suction surface to form a vortex street, in a manner similar to other bluff bodies. At low incidences the shear-layer separation point on the suction surface is located at the trailing edge of the aerofoil. As with a circular cylinder, this shear-layer separation point is not fixed, but will alter with incidence and Reynolds number because, by definition, this is the boundary-layer separation point on the aerofoil. Based on the comparison with the moving separation point for a circular cylinder, it is postulated that the upstream movement of the boundary-layer separation point will not eliminate any vortex shedding, but will affect the shedding process.

Principal Frequencies

Researchers investigating vortex shedding from bluff bodies such as plates and cylinders have observed that the shedding frequency reduces as the distance between two separating shear layers is increased.[15] This trend is consistent with the shedding process hypothesised by Gerrard[18] because increasing the distance between the two shear layers increases the time it takes for the opposite shear layer to cross the wake centerline and cut off the supply of vorticity from the rolling-up vortex. Increasing this time will increase the period of one shedding cycle and, hence, reduce the shedding frequency. This variation of shedding frequency with the distance between the two separating shear layers explains why f_p reduces as the height of the Gurney flap is increased, as is evident from the values listed in Table 1.

For bluff bodies there is also a relationship between the shedding frequency and the thickness of the separating shear layers. For a given mainstream velocity, the velocity gradient across a thicker boundary layer will be weaker and, hence, the vorticity lower. According to Gerrard,[18] this means that it will take longer for sufficient vorticity of opposing sign to cut off the supply to the rolling-up vortex. As a consequence, increasing the thickness of the shear layer will result in a reduction in shedding frequency. This effect could explain the reduction in principal frequency that is observed as the incidence of the wing is increased between $\alpha = +3$ and $+8$ deg. Although the trailing-edge suction and, hence, mainstream velocity at separation, remains broadly constant, the boundary-layer thickness increases with incidence. As a result the vorticity in the shear layer is weaker, and the shedding frequency reduces by a small amount.

For the wing fitted with a 4% Gurney flap there is a reduction in the shedding frequency between $\alpha = +8$ and $+10$ deg that is markedly larger than the changes observed for the same configuration between $\alpha = +3$ and $+8$ deg. Oil-flow visualizations revealed a region of separated flow at the trailing edge for $\alpha = +10$ deg, but not at $\alpha = +8$ deg. Such an upstream movement of the separation point between $\alpha = +8$ and $+10$ deg will increase the vertical distance between the two shear layers, which would explain the reduction in shedding frequency. Because this reduction is greater than those observed at lower incidences, it is postulated that changing the boundary-layer thickness has a weaker effect on the shedding frequency than increasing the vertical distance between the shear layers.

Trailing-Edge Suction

The results presented earlier showed that, for a given wing incidence and device height, the suction acting on the base of the Gurney flap remains constant across that face. Roshko[15] has shown that similar regions of constant suction are found between the separation points of bluff bodies caused by the vortex-shedding process. It appears, therefore, that the increased suction acting on the downstream face of the Gurney flap and, hence, acting at the trailing edge of the aerofoil, is enhanced by the vortex shedding.

While forming, the outer edges of the vortices entrain fluid from the base region, and this is balanced by a reverse flow into the base region between the two vortices. Bearman and Trueman[19] have proposed that it is this entrainment process that sustains the increased base suction, with a complex equilibrium between the vorticity shed by the body, the length of the recirculation region, and the base suction. Bearman[20] quantified the size of this recirculation region using the concept of the formation length l_f, which he defined as the axial distance from the base of the body to the position of maximum $\overline{u'^2}/U_\infty^2$. His results showed that if d/l_f was increased there was a near-linear reduction in the magnitude of the base suction.

Values of d/l_f derived from the LDA results are included in Table 1, along with values of the suction measured at the last tap on the aerofoil surface ($x/c = 0.96$), which gives a reasonable estimate of the trailing-edge suction. There is a loose relationship between these two parameters: Increasing the height of the Gurney flap increases both d/l_f and the trailing-edge suction, whereas the general trend for increasing the incidence is that both parameters are reduced. Note, however, that the changes in height of the Gurney flap result in small variations in d/l_f, but large variations in base suction, whereas altering the incidence has a more marked effect on the formation length, but with smaller changes in trailing-edge suction. It is, therefore, difficult to derive one relationship that fully explains the variation of trailing-edge suction with the height of the Gurney flap and the wing incidence.

Trailing-Edge Pressure

The chordwise pressures indicate that the Gurney flaps increase the pressure at the trailing edge of the aerofoil. This is caused by the upstream face of the Gurney flap decelerating the flow.

The results of Good and Joubert[21] for flat plates immersed in a turbulent boundary layer show that the maximum pressure measured upstream of the plate increases as the height of the disturbance is increased. These effects do not scale directly with device height, with the smaller plates causing a relatively large increase in pressure. For the results presented here, a similarly disproportionate increase in trailing-edge pressure is observed for the smaller Gurney flaps. It is, therefore, hypothesized that the upstream face of the Gurney flap acts like a bluff body on a ground plane: It decelerates the flow, which separates at some point upstream of the trailing edge, then reattaches at some point on the upstream face of the Gurney flap.

Chordwise Loadings

As discussed earlier, the Gurney flap introduces a pressure difference acting at the trailing edge of the aerofoil. Such a trailing-edge disparity can be modeled in a simple, two-dimensional panel model by modifying the implementation of the Kutta condition. Usually, this is modeled by setting the pressure coefficients at the trailing edge of the suction and pressure surfaces to be equal, using an equation of the form $\gamma_1 - \gamma_n = 0$, where γ_1 and γ_n are the singularity strengths for the trailing-edge panels on the different surfaces. This can be modified to account for a finite pressure difference at the trailing edge by setting the right-hand side of the preceding equation to some nonzero value $\Delta\gamma_{TE}$.

Typical results for a two-dimensional panel method with and without a pressure difference at the trailing edge are presented in Fig. 10.

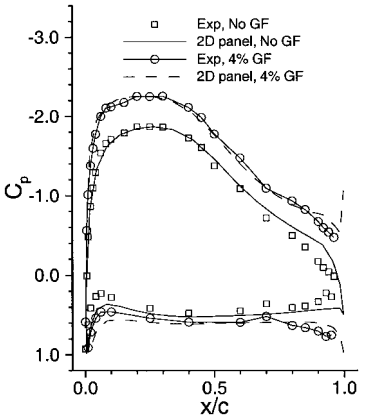

Fig. 10 Effect of trailing-edge pressure difference on loadings predicted by panel method.

This shows that introducing a finite pressure difference at the trailing edge generates an increase in loadings over the whole of the aerofoil. Such an increase in overall loadings has also been demonstrated computationally and experimentally by Kennedy and Marsden[22] for a single-element aerofoil designed to have a finite pressure difference at the trailing edge.

This increase in overall loading is unsurprising: the increase in suction-surface velocity and reduction in pressure-surface velocity caused by the Gurney flap can be treated conceptually as a point vortex placed at the trailing edge, which will increase the total circulation acting on the wing. This is analogous to the circulation effect by which a conventional slotted flap increases the lift of a wing, as first described by Smith.[10] Note that for a panel method that uses vortex singularities the equation used to introduce the pressure difference at the trailing edge explicitly introduces a point vortex because this is the right-hand term in the equation $\gamma_1 - \gamma_n = \Delta\gamma_{\mathrm{TE}}$.

The increase in maximum suction caused by this increase in circulation does not cause premature boundary-layer separation at low incidences because the increase in trailing-edge suction reduces the pressure recovery demands, as noted earlier. This effect can be compared to the increase in dumping velocity caused by a conventional slotted flap.[10]

Conclusions

The time-averaged flow downstream of a Gurney flap consists of two counter-rotating vortices, but the instantaneous flow structure actually consists of a wake of alternately shed vortices. The shedding frequency is related to the height of the Gurney flap and the boundary-layer thickness near the trailing edge of the aerofoil.

The vortex shedding sustains an increase in the base suction, which is near constant across the downstream face of the Gurney flap and is loosely related to the formation length of the recirculation region. The upstream face decelerates the flow, in a manner similar to a flat plate immersed in a turbulent boundary layer. The Gurney flap, therefore, introduces a pressure difference at the trailing edge, and it is this pressure difference that causes an increase in the total circulation.

Acknowledgment

The authors would like to thank Penske Cars Ltd., of Poole, Dorset, England, U.K., for funding this research program.

References

[1]Liebeck, R. H., "Design of Subsonic Airfoils for High Lift," *Journal of Aircraft*, Vol. 15, No. 9, 1978, pp. 547–561.

[2]Gruschwitz, E., and Schrenk, O., "Über eine Einfache Möglichkeit zur Auftiebserhöhung von Tragflügeln," *Zeitschrift für Flugtechnik und Motorluftschiffahrt*, No. 20, Oct. 1932, pp. 597–601.

[3]Duddy, R. R., "High Lift Devices and Their Uses," *Journal of the Royal Aeronautical Society*, Vol. 53, No. 465, 1949, pp. 859–900.

[4]Giguère, P., Lemay, J., and Dumas, G., "Gurney Flap Effects and Scaling for Low-Speed Airfoils," AIAA Paper 95-1881, June 1995.

[5]Myose, R., Papadakis, M., and Heron, I., "Gurney Flap Experiments on Airfoils, Wings, and Reflection Plane Model," *Journal of Aircraft*, Vol. 35, No. 2, 1998, pp. 206–211.

[6]Neuhart, D. H., and Pendergraft, O. C., Jr., "A Water Tunnel Study of Gurney Flaps," NASA TM-4071, Nov. 1988.

[7]Jang, C. S., Ross, J. C., and Cummings, R. M., "Computational Evaluation of an Airfoil with a Gurney Flap," AIAA Paper 92-2708, June 1992.

[8]Jeffrey, D., "An Investigation into the Aerodynamics of the Gurney Flap," Ph.D. Thesis, Dept. of Aeronautics and Astronautics, Univ. of Southampton, Southampton, England, U.K., July 1998.

[9]Eppler, R., *Airfoil Design and Data*, Springer–Verlag, Berlin, 1990, pp. 304, 305.

[10]Smith, A. M. O., "High-Lift Aerodynamics," *Journal of Aircraft*, Vol. 12, No. 6, 1975, pp. 501–530.

[11]Thompson, B. E., and Lotz, R. D., "Divergent Trailing-Edge Airfoil Flow," *Journal of Aircraft*, Vol. 33, No. 5, 1996, pp. 950–955.

[12]Simpson, R. L., Chew, Y. T., and Shivaprasad, B. G., "Structure of a Separating Turbulent Boundary Layer. Pt. 1. Mean Flow and Reynolds Stresses," *Journal of Fluid Mechanics*, Vol. 113, Dec. 1981, pp. 23–51.

[13]Cantwell, B., and Coles, D., "An Experimental Study of Entrainment and Transport in the Turbulent Near Wake of a Circular Cylinder," *Journal of Fluid Mechanics*, Vol. 136, Nov. 1983, pp. 321–374.

[14]Press, W. H., Teukolshy, A. S., Vetterling, W. T., and Flannery, B. P., *Numerical Recipes in FORTRAN*, Vol. 1, Cambridge Univ. Press, Cambridge, England, U.K., 1993, pp. 569–577.

[15]Roshko, A., "On the Drag and Shedding Frequency of Two-Dimensional Bluff Bodies," NACA TN-3169, July 1954.

[16]Coles, D., and Wadcock, A. J., "Flying-Hot-Wire Study of Flow Past an NACA Airfoil at Maximum Lift," *Journal of Aircraft*, Vol. 17, No. 4, 1979, pp. 321–329.

[17]Thompson, B. E., and Whitelaw, J. H., "Trailing-Edge Region of Airfoils," *Journal of Aircraft*, Vol. 26, No. 3, 1989, pp. 225–234.

[18]Gerrard, J. H., "The Mechanics of the Formation Region of Vortices Behind Bluff Bodies," *Journal of Fluid Mechanics*, Vol. 25, Pt. 2, June 1966, pp. 401–413.

[19]Bearman, P. W., and Trueman, D. M., "An Investigation of the Flow Around Rectangular Cylinders," *Aeronautical Quarterly*, Vol. 23, Pt. 3, Aug. 1972, pp. 229–237.

[20]Bearman, P. W., "Investigation of the Flow Behind a Two-Dimensional Body with a Blunt Trailing Edge and Fitted with Splitter Plates," *Journal of Fluid Mechanics*, Vol. 21, Pt. 2, Feb. 1965, pp. 241–255.

[21]Good, M. C., and Joubert, P. N., "The Form Drag of Two-Dimensional Bluff-Plates Immersed in Turbulent Boundary Layers," *Journal of Fluid Mechanics*, Vol. 31, Pt. 3, Feb. 1968, pp. 547–582.

[22]Kennedy, J. L., and Marsden, D. J., "The Development of High Lift, Single-Component Airfoil Sections," *Aeronautical Quarterly*, Vol. 30, Pt. 1, Feb. 1979, pp. 343–359.